Far East Journal of Electronics and Communications
Volume 10, Number 1, 2013, Pages 55-71
Published Online: May 2013
Available online at http://pphmj.com/journals/fjec.htm
Published by Pushpa Publishing House, Allahabad, INDIA

AMORPHOUS Ta_2O_5 MIM CAPACITORS PREPARED BY ELECTRON BEAM GUN

I. S. Yahia[1,2] **and Osama A. Azim**[3]

[1]Nano-Science and Semiconductor Labs.
Department of Physics
Faculty of Education
Ain Shams University
Roxy, Cairo
Egypt
e-mail: ihussein@kku.edu.sa
isyahia@gmail.com
dr_isyahia@yahoo.com

[2]Department of Physics
Faculty of Science
King Khalid University
P.O. Box 9004, Abha
Saudi Arabia

[3]Solar Energy Factory
Arab International Optronics Co.
El-Salam City, Cairo 1491
Egypt

Keywords and phrases: Ta_2O_5, electron beam gun, MIM capacitors, capacitance and dissipation factor, effect of temperature and frequency, Goswami and Goswami model, relaxation process.

Communicated by K. K. Azad

Received March 23, 2013

Abstract

Thin films of Ta_2O_5 have been fabricated by the direct electron beam gun evaporation technique, in an oxygen atmosphere. The capacitance of Ta_2O_5 MIM structure of thickness 666nm was determined. Ta_2O_5 thin film capacitors were studied at the temperature range (303-503K) and in the frequency range (100Hz-100kHz). Both of the measured capacitance C_m and dissipation factor $\tan\delta$ showed a pronounced dependence at the higher temperatures and lower frequencies. Goswami and Goswami (G-G) model was used to interpret the predicted characterization features of the measured capacitors and the dissipation factor as a function of temperature and frequency. The frequency dependence of the dissipation factor $\tan\delta$ at different temperatures shows a relaxation process. The results of the relative capacitance C_T/C_{RT} suggested the temperature and frequency dependencies. MIM of Ta_2O_5 is a good candidate for the dielectric capacitors for DRAM applications.

1. Introduction

The dielectric constant of dielectric thin films limits the degree of miniaturisation of capacitive components, which form the basis of many memory devices, such as DRAMs. All DRAM chips manufactured to date use capacitors containing dielectric films of SiO_2 and/or silicon nitride [1]. Capacitors dielectrics thinner than those now being used will suffer leakage due to Fowler-Nordheim tunnelling (around below 100Å). Many compounds with high dielectric constant are being widely investigated, including tantalum pentoxide (Ta_2O_5), which is already accepted in manufacturing facilities due to its compatibility with current microelectronics fabrication procedures. Metal-insulator-metal (MIM) capacitors are widely used in integrated circuits such as decoupling or fitter applications [2]. The Ta_2O_5 thin films as a dielectric layer have an exceptionally high dielectric constant and capacitors meeting the requirements for the new generation of memory devices and are also envisaged as a gate oxide in MOSFETs [3].

Thin films of Ta_2O_5 have been widely investigated as a potential dielectric material for use in DRAM capacitors due to the high dielectric constant and chemical stability. Ta_2O_5 is now in the closest position to practical application among a number of metal oxides and it might be utilized in high density DRAM with oxide equivalent thickness of about 5nm. (The equivalent oxide thickness refers to the thickness of any dielectric scaled by the ratio of its dielectric constant to that of SiO_2.) Usually, during the formation of Ta_2O_5, a silicon oxide layer is inevitably observed at the interface with Si. Its growth is favored by an oxidizing ambient at the beginning or during the fabrication step and by post-formation treatments performed in an oxygen atmosphere to repair the oxygen vacancies. The integration of Ta_2O_5 in the complete device fabrication process is still the subject of ongoing investigations [4].

On-chip integration of MIM capacitors is a key issue for high-performance technologies. MIM capacitor structures possess great importance as components of passive electronic devices in microprocessors and memories. Several single metal oxides have been commonly studied for the application in MIM structures, such as Al_2O_3, HfO_2, ZrO_2, Nb_2O_5, TiO_2 and Ta_2O_5 [5]. The integration of metal electrodes guarantees the accuracy and thermal stability of the capacitance value, its voltage independent behavior, and reduces the electrical resistance, making MIM capacitors fit the requirements of radio-frequency circuits, analog or mixed integrated circuits (ICs), and decoupling or memory applications [6, 7]. MIM capacitors using high dielectrics must be used in order to shrink the area for storage capacitor in dynamic random access memories [8].

In this work, the dielectric properties of Ta_2O_5 thin film capacitors were studied in details under the effect of frequency (100Hz-100kHz) and temperature (303-503K). The results are discussed according to Goswami and Goswami (G-G) model. The relaxation time and the relative capacitance are also calculated and interpreted.

2. Experimental

Tantalum pentoxide (Ta_2O_5) was supplied from Umicore Materials AG with purity 99.99%. Aluminum bottom electrodes were deposited onto very fine polishing and cleaning BK7 glass substrate as a coplanar geometry. Thin film of ditantalum pentoxide Ta_2O_5 was deposited onto pre-deposited BK7 substrate using electron beam gun system attached to high vacuum chamber type A700QE-Leybold Optics, Germany, at a pressure 8×10^{-6} mbar [9]. The glass substrate was held at room temperature RT. The adjusted evaporation rate was 0.5nm/s. The rate and final layer thickness were controlled by quartz crystal deposition monitor (model type IC/5). During the evaporation of the materials, the reactive process with oxygen O_2 was carried out at pressure 2.5×10^{-4} mbar [9].

The structural characterization of Ta_2O_5 thin film was investigated using X-ray diffraction pattern. Philips X-ray diffractometer (model X'-Pert) was used for the measurement of utilized monochromatic CuKα a radiation operated at 40kV and 25mA. The absence of any sharp diffraction peaks and the presence of hump emphasize the amorphous nature of the as-deposited film [9].

A programmable automatic RLC bridge (PM 6304 Fluke and Philips) was used to measure directly the impedance *Z*, the capacitance *C* and the loss tangent $(\tan \delta)$. All the investigated samples are represented on the screen of the bridge by a resistance *R* connected in parallel with a capacitance *C*. These measurements were achieved in the temperature range from (303-503K) and in the frequency range (100Hz-100kHz). The specimen was placed in a special designed holder to minimize the stray capacitance. Special designed holder was used for these measurements made from copper brass and the two electrodes are isolated from the base of the holder using two ceramic rings with screws.

3. Results and Discussion

3.1. Goswami and Goswami (G-G) model

The behavior of both the measured capacitance C_m and the dissipation factor $\tan\delta$ can be interpreted according to Goswami and Goswami (G-G) model [10]. In G-G model, each capacitor system is assumed to be comprised of a capacitance element *C*, which is unaffected by the frequency and temperature and a discrete resistance element *R* due to the dielectric film in parallel with *C*. Both *C* and *R* are in series with a resistance (bulk resistance) r_s, due to lead lengths (will be a constant during the measurements), …, etc as shown in Figure 1.

In the G-G model, it is assumed that $R(T)$ is a temperature-dependent according to the following equation [10-12]:

$$R(T) = R_0 \exp\left(\frac{-\Delta E_R}{k_B T}\right), \tag{1}$$

where R_0 is a constant, k_B is the Boltzmann's constant and ΔE is an activation energy, *T* is the absolute temperature. But a simple decrease of *R* is actually sufficient to explain the changed of the capacitance and loss tangent results under the effect of temperature and frequency. According to the G-G model, the measured capacitance C_m and the dissipation factor $\tan\delta$ can be expressed as [10-12]:

$$C_m = C_{\min} + \frac{1}{\omega^2 R^2 C_{\min}}, \tag{2a}$$

$$C_m = C_{\min} + \frac{1}{\omega^2 R\tau} \tag{2b}$$

and

$$\tan\delta \frac{\left(1 + \frac{r_s}{R}\right)}{\omega R C_{\min}} + \omega r_s C_{\min}, \tag{3}$$

where *R* is the interior resistance of the dielectric film, τ is the relaxation time, ω is the angular frequency and r_s is the bulk resistance. Equation (2) predicts that with increasing frequency, C_m should decrease and at high frequency, C_m should fall to a constant value $C_{\min}$ (the frequency independent capacitive element) which is very small. Also, for any frequency, C_m will increase with the increase of temperature because of the decreasing of interior resistance *R* (the dielectric film resistance). In equation (3), the expression for the dissipation factor predicts that at high frequency, the ω term is dominant while at low frequency, the term in ω^{-1} is dominant. So, equation (3) predicts a decrease in dissipation factor with increasing frequency at low frequency followed by a dissipation minimum at [10-12]:

$$\omega_{\min} = \frac{1}{C_{\min}\sqrt{rR}}, \quad (4)$$

and an increase in dissipation factor with increasing frequency at a certain high value of the frequency. But due to limitations of the RLC bridge, the minimum value could not be reached [12].

3.2. Frequency and temperature dependencies of the measured capacitance C_m of Ta_2O_5 thin films

To study the dielectric properties of Ta_2O_5 thin films, a coplanar (surface) device $Al/Ta_2O_5/Al$ [metal/insulator/metal] MIM was used. Figure 2(a) represents the measured capacitance C_m as a function of frequency in the range (100Hz-100kHz) and temperature in the range (303-503K). For temperatures approximately less than 393K, the capacitance is almost constant. After 393K, the measured capacitance C_m increases with the increase of temperature at lower frequency range [13-15]. The values of the minimum capacitance $C_{\min}$ at the higher frequency (100kHz) are shown in Figure 2(b). The values of $C_{\min}$ are increased with the increase of temperature.

The increase of the measured capacitance C_m in the high temperature-low frequency is probably due to space charge polarization induced by the increase of the number of free carriers as a result of increasing temperature [16, 17]. The observed increase of capacitance with temperature may be qualitatively explained by the equivalent circuit model developed by Goswami and Goswami [10] of bulk resistance r_s in series with parallel $R - C$ as shown in the stoichiometric circuit for the investigated Ta_2O_5 thin films as shown in Figure 1.

According to this model [10, 11], the measured capacitance C_m is interpreted according to equation (2). Accordingly, the increase of capacitance C_m with temperature may be due to the decrease of the interior resistance value of *R* with temperature [15] as given by equation (1).

From equation (1), an increase in the value of *T* implies a decrease of *R* and hence, an increase in the value of C_m from equation (2). This prediction is clearly illustrated at Figure 3. Furthermore, equation (2) also predicts that the measured capacitance should decrease with increasing the applied frequency reaching the minimum value of $C_{\min}$ at the higher studied frequency [11]. This effect can be illustrated by the plotting of C_m versus $\ln \omega$ as shown in Figure 4 for Ta_2O_5 thin film. This behavior may be due to the effect of charge redistribution by carrier hopping on defects [18, 19]. At the lower frequency, the charge on the defects can be rapidly redistributed, so that defects closer to the positive side of the applied field become negatively charged, while defects closer to the negative side of the applied field become positively charged. This leads to a screening of the field and an overall reduction in the electrical field because capacitance is inversely proportional to the field [20]. This leads to increase the capacitance. At the higher frequency, the defects have no longer enough time to rearrange inversions to the applied field; and hence, the capacitance decreases to the minimum value $C_{\min}$ as shown in Figure 4. It is observed that the high temperature is more effective on the carrier hopping because of the increase in the thermal emission of charges [20].

With the help of equations 2(a and b), the temperature and frequency dependencies of the dipole relaxation time τ can be determined. The temperature dependence of the dipole relaxation time τ at different frequency ranges (100Hz-2kHz) and (2kHz-20kHz) is shown in Figures 5(a and b), respectively. It is clear from these figures that relaxation time τ is approximately constant at low temperature and showed a pronounced increased at higher temperature while it decreased with the increase of the applied frequency. This behavior of τ is consistent with the temperature and frequency variations of the measured capacitance, i.e., at low frequencies and high temperatures, the mechanism of long relaxation time is dominant so capacity increases and vice versa, according to equation 2(a) [21].

The increase of the measured capacitance C_m with temperature, i.e., the increase of $\varepsilon'(\omega)$ with temperature can be attributed to the fact that the dipoles in polar materials cannot be oriented at low temperatures (remain frozen), while at high temperature, they can rotate freely as suggested by Srivastava et al. [22] and thus, increase the value of orientational polarization, and in turn increase $\varepsilon'(\omega)$. The decrease of $\varepsilon'(\omega)$ with frequency can be explained as follows [12]:

1. At low frequencies, the dielectric constant $\varepsilon'(\omega)$ for polar material is due to the contribution of multicomponent of polarizability, deformational polarization (electronic and ionic polarization) and relaxation polarization (orientational and interfacial polarization) [23].
2. When the frequency is increased, the dipoles will no longer be able to rotate sufficiently rapidly, so that their oscillations begin to lag behind those of the field.
3. As the frequency is further increased, the dipoles will be completely unable to follow the field and the orientation polarization stopped, so $\varepsilon'(\omega)$ decreases at higher frequencies approaching a constant value due to the interfacial or space charge polarization only.

3.3. Dissipation factor $\tan\delta$ as a function of frequency and temperature for Ta_2O_5 thin films

For an ideal parallel plate capacitor, no energy losses occur and the current leads the applied voltage by exactly 90°. In reality, the total current transversing such a capacitor is inclined by a power factor angle $\theta < 90^\circ$ against the applied voltage *V*. The main reason causing this type of behavior is the existence of internal capacitor resistance *R* in which, for an ideal capacitive element resistance equal to 0 Ω and this leads to the dissipation of power. Under these circumstances, the phase angle between current and voltage will be less than 90° and the loss factor $\tan\delta$ can be defined by [10-12]:

$$\tan\delta = \frac{1}{\omega R C_m} \tag{5}$$

or

$$\tan\delta = \frac{G}{\omega C_m}, \tag{6}$$

where $G = 1/R$ is the conductance of the device. Figures 6(a and b) illustrate the effect of temperature and frequency of the loss tangent $\tan\delta$ for Ta_2O_5 MIM device. It is clear from this figure that $\tan\delta$ increases with the increase of the applied frequency until it reaches its maximum approaches 13kHz and then it decreases with increasing the temperatures. This illustrates the relaxation process with a maximum curves peak of Ta_2O_5 thin film. Such behavior can be explained by G-G model [10]. According to this model [10, 11], the loss tangent $\tan\delta$ is interrupted by equation (3) as follows: at the lower frequency, $\tan\delta$ will decrease with increasing the frequency (ω^{-1} dominant term) followed by a minimum loss and then, an increase in the high frequency range (ω dominant term). As shown in Figures 6(a and b), the decrease of $\tan\delta$ with frequency is evident as predicted from equation (3) for the lower frequency and no indication of a minimum is observed over the investigated frequency range which may be due to the limitations of the frequency range of RLC bridge. However, further work is aimed to be extended for the measurements to the higher frequencies and temperatures employed in an attempt to observe the well-defined minima in $\tan\delta$ as predicted by the model of Goswami and Goswami. It is also hoped to investigate dielectric losses at very low frequencies for the investigated sample. Another prediction of equation (5) is the increase of $\tan\delta$ with increasing temperature as the ω^{-1} term becomes dominant term because of the decreasing value of R with temperatures [12].

3.4. The relative capacitance C_T/C_{RT}

The changes in the capacitance depend upon the area of the device, film thickness and dielectric properties of the investigated materials. In general form, the relationship between the relative dielectric constant, charge carrier concentration and polarizability of the material is determined by Clausius-Mosotti relation [24, 25]:

$$\frac{\varepsilon_{RT} - 1}{\varepsilon_{RT} + 2} = \frac{N_{RT}\alpha_{RT}}{3\varepsilon_0}, \tag{7}$$

where ε_{RT} is relative permittivity or dielectric constant under room temperature condition, ε_0 is permittivity of free space and N_{RT} is concentration of charge carriers at room temperature. From the above relation, we can derive:

$$\varepsilon_{RT} = \frac{(1 + (2N_{RT}\alpha_{RT}/3\varepsilon_0))}{(1 - (N_{RT}\alpha_{RT}/3\varepsilon_0))}. \tag{8}$$

Similar expression can be written for dielectric constant under different temperatures:

$$\varepsilon_T = \frac{(1 + (2N\alpha/3\varepsilon_0))}{(1 - (N\alpha/3\varepsilon_0))}. \tag{9}$$

The value of $N\alpha$ depends upon temperature. Relative capacitance-temperature relationship showed a logarithmic like behavior as shown in

Figure 7. The equation for $N\alpha$ can be written as:

$$N\alpha = N_{RT}\alpha_{RT}[1 + \log(1 + kJ)], \quad (10)$$

where k is thermo-capacitive factor, J is the temperature factor. By substitution using the value of $N\alpha$ in equation (9), we get

$$\varepsilon_T = \frac{(1 + (2N_{RT}\alpha_{RT}[1 + \log(1 + kJ)]/3\varepsilon_0))}{(1 - (N_{RT}\alpha_{RT}[1 + \log(1 + kJ)]/3\varepsilon_0))}. \quad (11)$$

From equations (8) and (11), we can derive the expression:

$$\frac{\varepsilon_T}{\varepsilon_{RT}} = \left(\frac{(1 + (2N_{RT}\alpha_{RT}[1 + \log(1 + kJ)]/3\varepsilon_0))}{(1 - (N_{RT}\alpha_{RT}[1 + \log(1 + kJ)]/3\varepsilon_0))}\right) \Big/ \left(\frac{(1 + (2N_{RT}\alpha_{RT}/3\varepsilon_0))}{(1 - (N_{RT}\alpha_{RT}/3\varepsilon_0))}\right). \quad (12)$$

At lower temperature, we may consider that:

$$(3\varepsilon_0 - N_{RT}\alpha_{RT}[1 + \log(1 + kJ)]) = 3\varepsilon_0 - N_{RT}\alpha_{RT}. \quad (13)$$

Now equation (12) can be written as:

$$\frac{\varepsilon_T}{\varepsilon_{RT}} = \left(\frac{(3\varepsilon_0 + 2N_{RT}\alpha_{RT}[1 + \log(1 + kJ)])}{(3\varepsilon_0 + 2N_{RT}\alpha_{RT})}\right). \quad (14)$$

The relation between dielectric constant and capacitance can be described by [26]:

$$\frac{C_T}{C_{RT}} = \left(\frac{\varepsilon_{temp.}}{\varepsilon_{RT}}\right)^n. \quad (15)$$

The factor n is related to dielectric (morphology). So, equation (14) can be modified as:

$$\frac{C_T}{C_{RT}} = \left(\frac{(1 + (2N_{RT}\alpha_{RT}[1 + \log(1 + kJ)]/3\varepsilon_0))}{(1 + (2N_{RT}\alpha_{RT}/3\varepsilon_0))}\right)^n. \quad (16)$$

According to equation (16), the relative capacitance C_T/C_{RT} is directly proportional with J (the temperature factor). The temperature dependence of the relative capacitance C_T/C_{RT} at different frequencies in the range (100Hz-100kHz) is shown in Figure 7. It is clear from this figure that the relative capacitance approximately increases exponentially with the increase of the temperature which agrees with equation (16). The increase of the capacitance with temperature can be attributed to the fact that the orientational polarization is connected with the thermal motion of molecules, so dipoles cannot orient themselves at low temperatures. When the temperature is increased, the orientation of dipoles is facilitated and this increases the value of orientational polarization and this increases the capacitance (i.e., dielectric constant) with increasing temperature [27].

4. Conclusions

MIM capacitors were prepared by the electron beam gun technique. The capacitance and the dissipation factor were interpreted using the equivalent circuit developed by Goswami and Goswami of bulk resistance r_s in series with parallel $R-C$ for the high dielectric Ta_2O_5 thin film. The dissipation factor showed a relaxation process. It is found that the relative capacitance is increased with increasing the temperature and decreased with increasing the applied frequency. It is suggested to use Ta_2O_5 thin film on various capacitance electronic devices instead of SiO_2. Ta_2O_5 film as a dielectric layer shows the high capacitance meeting the requirements for the new generation of memory devices.

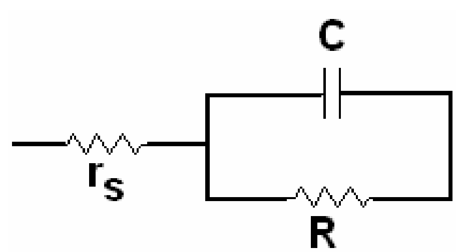

Figure 1. Schematic diagram of G-G model.

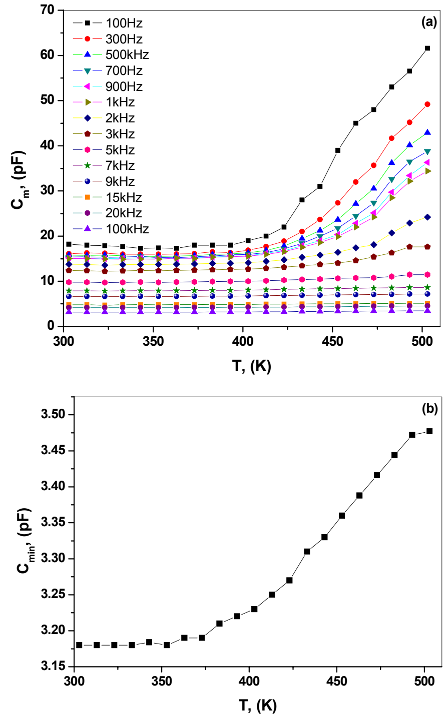

Figures 2(a and b). (a) Temperature dependence of the measured capacitance C_m at different frequencies of Ta_2O_5 MIM device. (b) Temperature dependence of the minimum values of the capacitance $C_{\min}$ at 100kHz.

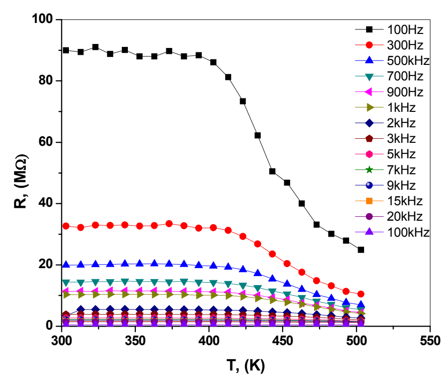

Figure 3. The frequency dependence of the resistance R at different temperatures of the investigated MIM device.

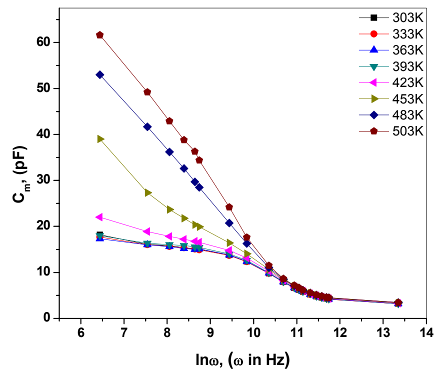

Figure 4. Frequency dependence of the measured capacitance C_m at different temperatures of Ta_2O_5 MIM device.

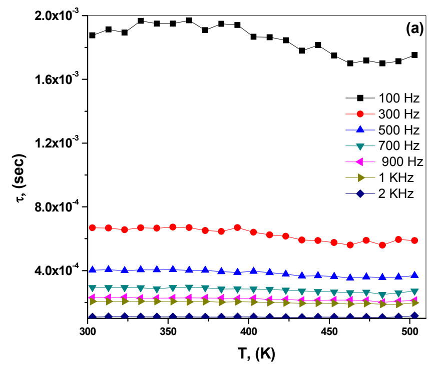

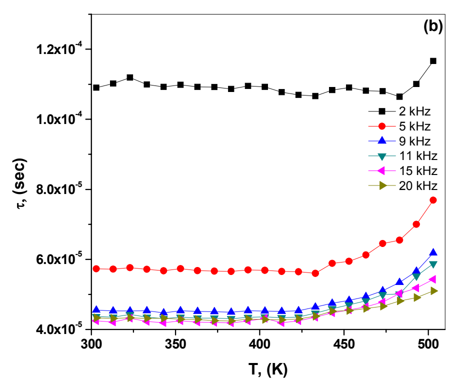

Figures 5(a and b). Temperature dependence of the relaxation time τ of Ta_2O_5 MIM device at different frequencies.

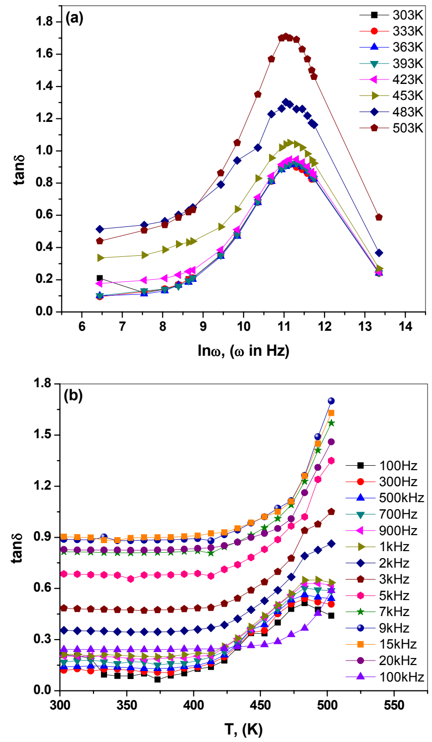

Figures 6(a and b). (a) Frequency dependence of the dissipation factor $\tan\delta$ at different temperatures of Ta_2O_5 MIM device. (b) Temperature dependence of the dissipation factor $\tan\delta$ at different frequencies of Ta_2O_5 MIM device.

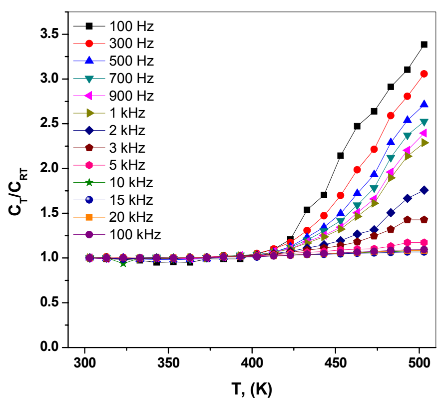

Figure 7. The relative capacitance-temperature relationships for $Al/Ta_2O_5/Al$ MIM device.

References

[1] A. Cappellani, J. L. Keddie, N. P. Barradas and S. M. Jackson, Solid-State Electronics 43 (1999), 1095-1099.

[2] A. Bajolet, R. Clerc, G. Pananakakis, E. Picollet, N. Segura, S. Boret, S. Bruyère, J. P. Manceau, J. C. Giraudin, P. Delpech, L. Montès and G. Ghibaudo, Solid-State Electronics 50 (2006), 1244-1251.

[3] C. Chaneliere, S. Four, J. L. Autran and R. A. B. Devine, Microelectronics Reliability 39 (1999), 261-268.

[4] E. Atanassova and A. Paskaleva, Microelectronics Reliability 42 (2002), 157-173.

[5] E. Gerritsen, N. Emonet, C. Caillat, N. Jourdan, M. Piazza, D. Fraboulet, B. Boeck, A. Berthelot, S. Smith and P. Mazoyer, Solid-State Electron 49 (2005), 1767.

[6] A. Farcy, J. Torres, V. Arnal, M. Fayolle, H. Feldis, F. Jourdan, M. Assous, J. L. Di Maria and V. Vidal, Microelectronic Engineering 70 (2003), 368-372.

[7] J. A. Babcock, S. G. Balster, A. Pinto, C. Dirnecker, P. Steinmann, R. Jumpertz and B. El-Kareh, IEEE Electron Dev. Lett. 22 (2001), 230.

[8] Y. Matsui, Y. Nakamura, Y. Shimamoto and M. Hiratani, Thin Solid Films 437 (2003), 51-56.

[9] Azima A. Osama, M. M. Abdel-Azizb and I. S. Yahia, Appl. Surf. Sci. 255 (2009), 4829-4835.

[10] A. Goswami and P. Goswami, Thin Solid Films 16 (1973), 175.

[11] Anthopoulos D. Thomas and Shafai S. Torfeh, J. Appl. Phys. 94 (2003), 2426.

[12] Ibrahim Sayed Mohammed Hussein, (I. S. Yahia), Ph.D. Thesis, Physics Department, Faculty of Education, Ain Shams University, Cairo, Egypt, 2007.

[13] J. C. Anderson, Dielectrics, Reinhold, New York, 1964.

[14] M. El-Shabasy and A. S. Riad, Physica B 222 (1996), 153.

[15] M. A. M. Seyam, Appl. Surf. Sci. 181 (2001), 128.

[16] H. S. Nalwa and P. Vasudevan, J. Mater. Sci. Lett. 2 (1983), 71.

[17] R. D. Gould and A. Hassan, Thin Solid Films 223 (1993), 334.

[18] P. W. Zukowski, S. B. Kantorow, D. Maczka and V. Stelmakh, Phys. Stat. Sol. (a) 112 (1989), 695.

[19] A. Vasudevan, S. Carin, M. R. Melloch and E. S. Harmon, Appl. Phys. Lett. 73 (1998), 671.

[20] A. M. A. El-Barry and H. Atyia, Physica B 368 (2005), 1.

[21] S. Yildirim, K. Ulutas, D. Deger, E. O. Zayim and I. Turhan, Vacuum 77 (2005), 329-335.

[22] K. K. Srivastava, A. Kumar, O. S. Panwar and K. N. Lakshminarayan, J. Non-Cryst. Solids 33 (1979), 205.

[23] B. Tareev, Physics of Dielectric Materials, Mir Publishers, Moscow, 1975, p. 42.

[24] M. Omar Ali, Elementary Solid State Physics: Principles and Applications, Published by Pearson Education (Singapore), Pte. Ltd., 2002.

[25] M. H. Sayyed, M. Shah, K. S. Karimov, Z. Ahmad, M. Saleem and M. Tahir Maroof, Journal of Optoelectronics and Advanced Materials 10 (2008), 2805- 2810.

[26] Z. M. Rittersma, Sensors and Actuators A 96 (2002), 196-210.

[27] A. E. Bekheet, Physica B 403 (2008), 4342-4346.